Wang, M. and Chen, Q. "On a hybrid RANS/LES approach for indoor airflow modeling, Accepted by *HVAC&R Research*.

On a Hybrid RANS/LES Approach for Indoor Airflow Modeling

This paper is based on findings resulting from ASHRAE Research Project RP-1271.

Miao Wang[1] *Student Member ASHRAE*

Qingyan (Yan) Chen, Ph.D. *Fellow ASHRAE*

ABSTRACT

The airflows in an enclosed environment are a wall bounded unstable flow, which is difficult to simulate using either a RANS or a LES model. The hybrid RANS/LES simulation, which uses a RANS model for the near wall attached boundary layers to avoid an excessively fine grid, and a LES for the separated turbulence region to resolve unstable eddies, are promising for this type of flow. However, the available hybrid RANS/LES models have not performed well for indoor airflows due to the RANS model they used. This investigation developed a new RANS/LES model for indoor airflow modeling using a semi-v2f model. This model predicted correctly near-wall flows by taking into account the wall normal stress, which was calculated by an algebraic equation. By applying the new model to a mixed-ventilation flow in a room and a strong buoyancy-driven flow with a high temperature gradient in a room, the predicted results are accurate and the model seems robust.

ACRONYMS

ACH	=	Air Changes per Hour	N-S	=	Navier-Stokes
CFD	=	Computational Fluid Dynamics	RANS	=	Reynolds-Averaged Navier-Stokes equations
DES	=	Detached Eddy Simulation	Re	=	Reynolds Number
DES-SA	=	Detached Eddy Simulation with Spalart-Allmaras model	RMS	=	Root-Mean-Square
DNS	=	Direct Numerical Simulation	S-A	=	Spalart-Allmaras
LDV	=	Laser Doppler Velocimetry	SST	=	Shear Stress Transport
LES	=	Large Eddy Simulation	v2f	=	The v2f model
LES-DSL	=	Large Eddy Simulation with Dynamic	v2f-Dav	=	v2f model modified by Davidson

[1] Mr. Miao Wang is a Research Assistant and Qingyan Chen is a Professor at School of Mechanical Engineering, Purdue University, Indiana

Smagorinsky-Lilly model

SYMBOLS

A	=	Model constant	l^*	=	No-dimensional distance to the wall
C	=	Model constant	R	=	Gas constant
D^k_{RANS}	=	Dissipation term in the SST k-ω model	P	=	Pressure
d_w	=	Distance to the nearest wall	S_{ij}	=	Strain rate tensor
G	=	Filter function for LES	T	=	Temperature
k	=	Turbulence kinetic energy	u	=	Velocity
L	=	Size of the test room	$\overline{v'^2}$	=	Wall normal stress
l	=	Turbulence length scale	x, y, z	=	Cartesian coordinates
$\tilde{l}$	=	DES blending function	$y*$	=	$\frac{yC_\mu^{1/4}k^{1/2}}{\nu}$

GREEK SYMBOLS

Δ	=	Grids spacing	σ	=	Model constant
δ_{ij}	=	Kronecker delta	τ_{ij}	=	For RANS: $-\overline{u_i'u_j'}$ For LES: $\overline{u_i}\,\overline{u_j}-\overline{u_iu_j}$
ε	=	Turbulence dissipation rate	Φ	=	Mean flow variables
ν	=	Kinematic viscosity	ϕ	=	Flow variables
$\tilde{\nu}$	=	Modified turbulence viscosity	ω	=	Specific turbulence dissipation rate
ρ	=	Density			

SUBSCRIPTS

DES	=	Detached eddy simulation	min	=	Minimum value
i	=	The i-th direction	op	=	At the opening
j	=	The j-th direction	RANS	=	The RANS model
LES	=	Large eddy simulation	RKE	=	The RANS k-ε model
max	=	Maximum value	t	=	Turbulence quantities

OVERBARS

Over bar	=	Mean and filtered flow variables for RANS and LES respectively	Tilde	=	Variables for DES-SA model

1 EQUATION SECTION (NEXT)INTRODUCTION

Airflow in enclosed spaces can be complicated due to complex flow features such as flow transition and lack of stability. Many indoor airflows are transitional when the Reynolds number based on the supply air grille is in the region of 2000< Re <3500. Turbulence is generated at the grille where the fluctuating component of velocity is a fraction of the mean velocity. As the air travels further into the room, the fluctuating component may decay gradually due to the decrease in the mean flow gradient and damping effect of the solid surfaces. Therefore, relaminization may occur within the occupied space, and the flow is transitional. In addition to flow transition, in many indoor environments, airflow with relatively high air change rates (between 5 to 20 ACH) can be unstable under the transitional Reynolds number. One reason for this is that the transitional phenomenon makes the flow unstable. In the transitional region, the inertial force is approximately balanced by the viscous force. A random small impact from the main stream can break down this balance and lead to a transitional flow. This mechanism results in the instability of the main flow. Another reason attributed to the unstable flow is the interaction between different flow features. Many enclosed environments are mechanically ventilated. However, the air can also be driven by buoyancy in the occupied zone, where the thermal plume can be as strong as the flow from the mechanical ventilation system. The two flows interact, and result in instability. Besides, the complex geometry of the indoor environment can also lead to an unstable flow. The furniture inside an indoor environment can generate flow separation, which is usually unstable. As discussed above, the flow transition and unstable behaviors cause complicated indoor airflow phenomena, making indoor airflow difficult to model.

To model indoor airflow, one approach is to apply Computational Fluid Dynamics (CFD) to solve the flow equations. The airflow in a room is governed by the Navier-Stokes (N-S) equation. The most straightforward way to solve this equation is called Direct Numerical Simulation (DNS), which directly solves the N-S equation together with initial and boundary conditions and produces a realization of the flow. The DNS does not need any model and can provide the most accurate and detailed flow motion. However, the DNS resolves a wide range of spatial and temporal scales, from the smallest Kolmogorov scale (scale of dissipative eddies) to the integral scale (scale large flow motion), which requires a very fine meshes and time steps (Wilcox 2006). Even for steady-state flow, DNS needs to perform unsteady calculation, and calculate a long period of time to obtain the mean flow. As a result, the cost of DNS can be extremely high. For example, to simulate a small office under mechanical ventilation with the Reynolds number of 5000, the grid spacing should be in the order of 10^{-3} m (Kolmogorov length scale). The number of cells for the room is in the order of 10^{10}. The size of the time step should be in the order of 10^{-3} s (Kolmogorov time scale). To obtain a sufficient statistical sample, the flow should be calculated for several minutes. Therefore, the number of time steps should be in the order of 10^{6}.

However, it is not feasible to perform the simulation on a personal computer or a moderate computer cluster in the near future.

A more realistic and widely used approach for indoor airflow simulations is by the Reynolds-Averaged Navier-Stokes (RANS) equation modeling. The RANS simulation solves the time-averaged N-S equation and models the additional Reynolds stresses. The modeling approach can significantly reduce the grid resolution requirement, and can be performed as steady-state. Many studies have used different RANS models for indoor airflow simulation (Yuan et al. 1999, Holmes et al. 2000, Gadgil et al. 2003, Hsieh and Lien 2004, Zhang et al. 2007) and found mixed results of the model performance. Zhang et al. (2007) tested eight popular turbulence models for different indoor airflows and concluded that no model was superior to other models. Wang and Chen (2009) further tested these eight models using a set of experimental cases with gradually added flow features and found that the RANS models failed to predict flow separation. This conclusion was supported by Costa et al. (1999) to some extent, who found that the low Reynolds number model suffered from singular problem, leading to the prediction of an unrealistic local minimum of the wall heat transfer near points of flow reattachment. The failure of the RANS models to predict a separated flow could have resulted from the time-averaging approach. In the separation region, the flow is very unstable, and the velocity magnitude and direction change rapidly. Therefore, it may not be meaningful to have a time-averaged solution for this case since the information contained by the mean value of flow variables is too limited to describe the rapidly varying unstable flow. Thus, the RANS models may not be capable of correctly predicting unstable airflow features in enclosed spaces, such as the separation caused by furniture, impinge flow, and unsteady plumes.

With the advancement of computing power, the Large Eddy Simulation (LES) is becoming more and more popular for engineering applications due to its ability to solve the unstable separated flow. LES solves the filtered N-S equation for the energy containing eddies (large eddies) and models the subgrid-scale flow motions (small eddies). The turbulence model for LES is not as important as that for a RANS model (Wang and Chen, 2009). In other words, LES relies more on fundamental flow physics than on modeling assumptions. As a result, LES is more accurate and informative than RANS models for airflow modeling, especially for a separated and unstable flow. Since LES solves only the large scale eddies, the computing cost is much lower than that of DNS. The cell size required by LES could be much larger than the Kolmogorov length scale. Therefore, LES uses significantly less computational time than DNS. For example, to calculate a flow over a backward-facing step by DNS (Le et al., 1997) and by LES (Akselvoll and Moin, 1993) at Reynolds number of 5000, the LES requires only 3% of the cells and 2% of the computing time needed by the DNS, while having an equally good results compared with the experimental data (Wilcox, 2006). However, it is difficult to apply LES for the near wall region of indoor airflow modeling, where the size of the energy-bearing eddies (large eddies) is comparable to that of the dissipative eddies. If LES is to resolve most energy bearing eddies, the computing cost could be the same as that of the DNS. For airflow in

enclosed spaces, the flow is bounded by walls, furniture, and occupants. All of these solid surfaces could significantly increase the computing cost by LES.

To overcome the disadvantages of the LES and RANS, the concept of the RANS/LES hybrid model has emerged in the past decade. The hybrid model is to apply LES in the separated flow region to capture the three-dimensional, time-dependent flow and to apply a RANS model in the attached boundary layers so as to avoid the excessively fine meshes required by LES. This approach was first introduced by Spalart et al. (1997), adopting the one equation Spalart model. Some studies used Smagoringsky zero-equation LES model with zero-equation RANS model such as Cebeci-Smith and Baldwin-Lomax models (Georgiadis et al., 2003; Kawai and Fujii, 2005). Many other studies adopted multi-equation RANS models with LES, such as k-ω model (Strelet 2001; Davidson and Peng 2003), k-ε model (Hamba 2001, 2003), and k-l model (Tucker and Davidson 2004). After reviewing the RANS/LES hybrid models, our effort was to develop a new hybrid model, the Semi-v2f/LES model, for modeling airflows in an enclosed environment. The new model used transport equations for k and ε, and an algebraic equation for the normal stress near a wall to model the turbulence viscosity in the RANS region, and the subgrid turbulence viscosity for the LES region. The new model was tested by applying to a mixed convection flow in a model room, and to a strong buoyancy-driven flow with a high temperature gradient in a room.

2 EQUATION SECTION (NEXT)MODEL DEVELOPMENT

2.1 Hybrid RANS/LES Simulation for Indoor Airflow

Indoor airflow is governed by the N-S equation. Since it is not feasible to use DNS for solving such a flow, the N-S equation should be approximated in order to make it solvable with the present capacity of computers. By using Reynolds averaged approach, flow variables can be written as:

$$\phi = \Phi + \phi' \tag{2.1}$$

where, Φ is the mean value of flow variables, and ϕ' is the fluctuating part of flow variables. On the other hand, LES uses a filter to obtain large-scale flow variables:

$$\overline{\phi}(\vec{x},t) = \iiint_V \phi(\vec{x},t) G(\vec{x},\vec{x}',t) d\vec{x}' \tag{2.2}$$

where the over bar denotes the filtered variables, and G is a filter function.

The two methods can transform the N-S equation into a single form:

$$\frac{\partial \overline{u_i}}{\partial x_i} = 0 \tag{2.3}$$

$$\frac{\partial \overline{u_i}}{\partial t} + \overline{u}_j \frac{\partial \overline{u_i}}{\partial x_j} = -\frac{1}{\rho}\frac{\partial \overline{P}}{\partial x_i} + \nu \frac{\partial^2 \overline{u_i}}{\partial x_j \partial x_j} + \frac{\partial \tau_{ij}}{\partial x_j} \tag{2.4}$$

where the over bar denotes mean variables for RANS, and filtered variables for LES. The term τ_{ij} in the equation is the Reynolds stress for RANS:

$$\tau_{ij} = -\overline{u_i' u_j'} \tag{2.5}$$

and the subgrid-scale stress for LES:

$$\tau_{ij} = \overline{u_i u_j} - \overline{u_i}\,\overline{u_j} \tag{2.6}$$

Many turbulence models use Boussinesq approximation to simplify the second order symmetrical tensor by correlating it to a scalar ν_t, and transform equation (2.4) into:

$$\frac{\partial \overline{u_i}}{\partial t} + \overline{u}_j \frac{\partial \overline{u_i}}{\partial x_j} = -\frac{1}{\rho}\frac{\partial \overline{P}}{\partial x_i} + \frac{\partial}{\partial x_j}\left[\left(\nu + \nu_t\right)\frac{\partial \overline{u_i}}{\partial x_j}\right] \tag{2.7}$$

where ν_t is the turbulence viscosity for the RANS model and the subgrid-scale turbulence viscosity for LES.

Spalart et al. (1997) introduced the first hybrid RANS/LES method, named Detached Eddy Simulation Spalart-Allmaras (DES-SA) model. This model used the Spalart-Allmaras one-equation model to calculate the turbulence viscosity for the RANS part and modified the length scale in the equation to calculate the subgrid-scale turbulence viscosity for the LES part. The transport equation for $\tilde{\nu}$ is written as:

$$\frac{\partial \tilde{\nu}}{\partial t} + \overline{u}_j \frac{\partial \tilde{\nu}}{\partial x_j} = c_{b1}\tilde{S}\tilde{\nu} - c_{w1} f_w \left(\frac{\tilde{\nu}}{\tilde{l}}\right)^2 + \frac{1}{\sigma}\frac{\partial}{\partial x_k}\left[\left(\nu + \tilde{\nu}\right)\frac{\partial \tilde{\nu}}{\partial x_k}\right] + \frac{c_{b2}}{\sigma}\frac{\partial \tilde{\nu}}{\partial x_k}\frac{\partial \tilde{\nu}}{\partial x_k} \tag{2.8}$$

where $\tilde{\nu}$ is the modified turbulence viscosity used as a working variable. c_{b1}, c_{b2}, c_{w1}, and σ are constants, and

$$\begin{aligned} \tilde{l} &= \min(d_w, C_{DES}\Delta) \\ \Delta &= \max(\Delta x, \Delta y, \Delta z) \end{aligned} \tag{2.9}$$

The $\tilde{l}$ is the DES-blending function. In Eq. (2.9) d_w is the distance to the nearest wall, and also the RANS length scale used by the S-A model, the C_{DES} is a constant and the Δ is the largest cell spacing. The $C_{DES}\Delta$ represents the grid length scale. The $\tilde{l}$ compares the RANS length scale with the grid length scale. If the cell is close to the wall, i.e. the wall distance is smaller than the grid size, the DES-blending function is equal to the wall distance, and the transport equation has the same form as the Spalart-Allmaras model. Otherwise, the equation becomes a "Smagorinsky-like" subgrid-scale turbulence viscosity based on the local grid size.

Many hybrid models with more advanced RANS models have been developed based on the idea of the DES-SA model (Hamba 2001; Strelet 2001; Tucker and Davidson 2004). One can replace explicitly the d_w in the DES-SA model by the turbulence length scale or implicitly involved in other RANS models. Strelet (2001) developed a RANS/LES hybrid model based on Menter's (2003) SST k-ω model. The major modification was on the dissipation term in the SST k-ω model:

$$D_{RANS}^{k} = \rho k^{3/2} / \tilde{l} \tag{2.10}$$

where:

$$\tilde{l} = \min(l_{k-\omega}, C_{DES}\Delta) \tag{2.11}$$

The $C_{DES}\Delta$ was the same as that in the DES-SA model. Note that the RANS scale used in this model is the turbulence length scale, which means the switching between the RANS and LES mode is based on the local eddy size and local grid size.

The hybrid RANS/LES models are usually classified based on the RANS model they use. The performance of a hybrid RANS/LES model also depends on its RANS model. For indoor airflow simulation, a few preliminary studies in the literature show that the available RANS/LES hybrid models did not perform as well as LES or even as well as some RANS models. This is because the RANS models used were not good (Zhang et al. 2007; Wang and Chen, 2009). Therefore, our effort was to identify an appropriate RANS model for indoor airflow simulations and to develop a new hybrid model with the RANS model.

2.2 Identification of a Suitable RANS Model for Hybrid Simulation

As discussed above, the accuracy of the RANS model is essential to the performance of a hybrid model. Some studies have evaluated different RANS turbulence models for indoor airflow, which could be helpful for choosing a suitable RANS model. Zhai et al.

(2007) identified a total of 17 models that may be appropriate for calculating indoor airflows. Wang and Chen (2009) tested six of them that are most promising for indoor airflows and concluded that the v2f model, the RNG k-ε model, and the Reynolds stress model were the best. This conclusion was consistent with that from Zhang et al. (2007) for forced, natural, and mixed convection flows.

Since the RNG k-ε model uses a wall function near solid boundaries, which makes it unsuitable for a hybrid model. The Reynolds stress model can resolve the near wall region, but it has six scalar transport equations that are too computationally expensive. The v2f model can be used for the hybrid model since it can resolve the near wall viscous region at a reasonable computational cost (three scalar transport equations), and accounts for anisotropic behavior near the wall. However, studies from the literature (Durbin, 1991, Davidson, 2003) and our preliminary research show that the transport equation for the wall normal stress $\overline{v'^2}$ and the elliptic equation for the relaxation function f make the model numerically unstable. Therefore, it is essential to simplify the v2f model before implementing it in a hybrid simulation.

2.3 The Semi-v2f/LES Model

Our effort to develop the v2f model further was to introduce an algebraic equation for the normal stress $\overline{v'^2}$:

$$\overline{v'^2} = f\left(k,\varepsilon,\upsilon,y...\right) \tag{2.12}$$

to replace the transport equation for $\overline{v'^2}$ and the elliptic equation for f, which have been problematic. The procedure was first to derive new equations for $\overline{v'^2}$ and turbulence viscosity. The constant in the equations was then determined through curve fitting of the flow data obtained for indoor airflow. The detailed procedure was as follows.

$\overline{v'^2}$ equation

Starting from the Buossinesq approximation for incompressible flow:

$$-\tau_{ij} = -2\nu_t S_{ij} + \frac{2}{3}k \cdot \delta_{ij} \tag{2.13}$$

considering the diagonal entries at wall normal direction (i=j=2), and substituting the ν_t formulation of v2f model, it is easy to obtain a correlation:

$$\frac{\overline{v'^2}}{k} = C_1\left(1 - C_2\frac{\overline{v'^2}}{\varepsilon}\frac{\partial V}{\partial y}\right) \tag{2.14}$$

where C_1 and C_2 are constants. Through dimensional analysis of equation (2.14), there are three non-dimensional variables: $\frac{\overline{v'^2}}{k}$, $y^* = \frac{yC_\mu^{1/4}k^{1/2}}{\nu}$, and $l^* = \frac{k^{\frac{3}{2}}}{\varepsilon y}$. Therefore, equation (2.14) can be written as a dimensionless form:

$$\frac{\overline{v'^2}}{k} = C_1\left[1 - g\left(y^*, l^*\right)\right] \tag{2.15}$$

where $g\left(y^*, l^*\right)$ g is the function to be determined. If the y* value becomes large (far from the wall), the turbulence should be homogeneous:

$$\frac{\overline{v'^2}}{k} = C_1\left[1 - g\left(y^*, l^*\right)\right] \xrightarrow{y^* \to \infty} C_1 \tag{2.16}$$

Near a wall, the normal kinetic energy goes to zero:

$$\frac{\overline{v'^2}}{k} = C_1\left[1 - g\left(y^*, l^*\right)\right] \xrightarrow{y^* \to 0} 0 \tag{2.17}$$

Assuming the wall damping effect only related to the geometry, the influence of l^*, which was the turbulence eddy scale, could be neglected. Thus, equations (2.16) and (2.17) could be a good approximation of equation (2.14). Namely:

$$\frac{\overline{v'^2}}{k} = C_1\left[1 - \exp\left(-\frac{y^*}{y^*_0}\right)\right] \tag{2.18}$$

where C_1 and y^*_0 are constans.

Turbulence Viscosity

In the v2f model, the turbulence viscosity is modeled as:

$$\nu_t = C_\mu \overline{v'^2}\frac{k}{\varepsilon} \tag{2.19}$$

where, $C_\mu = 0.22$ is a constant. By Substituting equation (2.18) into equation (2.19), the turbulence viscosity can be determined by:

$$\nu_t = A \cdot \left[1 - \exp\left(-\frac{y^*}{y^*_0}\right)\right] \cdot \frac{k^2}{\varepsilon} \tag{2.20}$$

where A and y^*_0 are constant to be determined.

Determination of Constant

The model derived above was to mimic the behavior of the v2f model. Therefore, this study simulated several room airflows using the v2f model, extracted the data from different locations, and performed a curve fitting on equation (2.18) to determine the constants. The curve fitting results led to the new algebraic $\overline{v'^2}$ equation:

$$\frac{\overline{v'^2}}{k} \approx 0.308\left[1 - \exp\left(-\frac{y^*}{50.836}\right)\right] \tag{2.21}$$

and the turbulence viscosity:

$$\nu_t = 0.07\left[1 - \exp\left(-\frac{y^*}{50.836}\right)\right] \cdot \frac{k^2}{\varepsilon} \tag{2.22}$$

Figure 1 compares the $\overline{v'^2}/k$ near the wall by the algebraic equation with the DNS data (Alamo et al., 2004). The agreement is reasonably well.

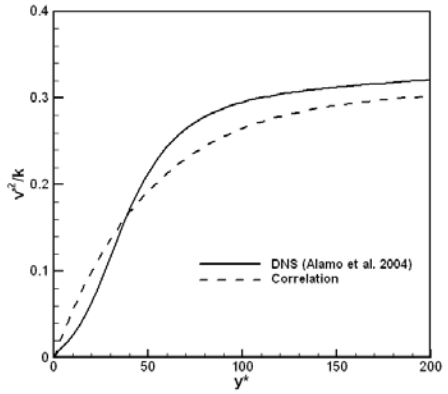

Figure 1 Comparison between the algebraic correlation and the DNS data.

New Semi-v2f/LES Model

The new Semi-v2f/LES model used the same k and ε equations as those in the DES realizable k-ε model, but had a new algebraic equation for $\overline{v'^2}$ and a new eddy-viscosity correlation. The appendix provides more detailed formulation of the Semi-v2f/LES model.

3 EQUATION SECTION (NEXT)PERFORMANCE OF THE SEMI-V2F/LES MODEL

This study evaluated the performance of the Semi-v2f/LES model by applying it to two benchmark cases: a mixed convection flow in a model room with moderate buoyancy (Wang and Chen 2009) and a strong buoyancy-driven flow in a model fire room (Murakami et al. 1995). The first case had a simple geometry but most features of indoor airflow. The second case was selected to test the robustness of the new model in an extreme scenario.

3.1 Mixed convection Flow

Figure 2 (a) shows the case schematic. The air velocity distributions were measured at the stream-wise and the cross sections in the 8 x 8 x 8 ft (2.44 x 2.44 x 2.44 m) cubic room. The air was supplied from a slot diffuser located at the upper-left corner of the room, and exhausted from a slot at the lower-right corner. The Reynolds number based on the inlet height was about 2500, which was in the transitional region. A 4 x 4 x 4 ft (1.22 x 1.22 x 1.22 m) heated box was placed in the center with 700 W of power, which produced a thermal plume. The box also caused flow separation. This case represents a typical indoor airflow scenario with most important flow features. Please find more information about this case from Wang and Chen (2009).

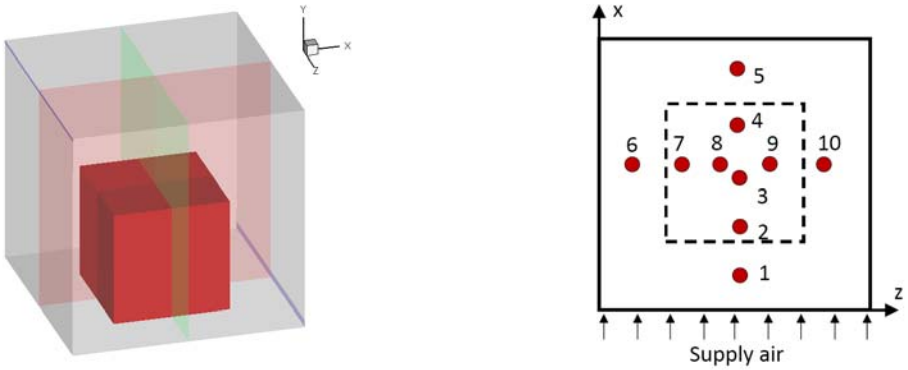

(a) (b)

Figure 2 A mixed convection flow in a room (Wang and Chen 2009): (a) the case schematic and the measuring section locations and (b) ten positions selected for comparison between the new model results and the experimental data.

The Semi-v2f/LES model was implemented into FLUENT (Fluent 2003) by user-defined functions. According to Wang and Chen (2009), two grid resolutions were used for the new model: one was a 44x44x44 grid (coarse); the other was a 110x77x101 grid (fine). The v2f model modified by Davidson (v2f-Dav) (2003), the LES Dynamic Smagorinsky-Lilly (LES-DSL) model, and the DES Realizable k-ε model were also included in this study to evaluate the performance of the new model. The LES-DSL model and DES Realizable k-ε model used a 110x77x101 grid and the v2f-Dav model used a 44x44x44 grid. The comparison was based on the velocity, temperature, and turbulence kinetic energy at ten positions as shown in Figure 2 (b). The results shown in this paper were at the positions where turbulence models had the best, worst, and average performances. Please refer toWang and Chen (2009) for the definition of the three categories.

Figure 3 depicts the air velocity prediction by the four models. In general, all the models predicted very similar, acceptable results. The new model slightly under-predicted the velocity at position (6) with a fine grid. The Realizable k-ε had a similar prediction at this position. However, the discrepancy was very small. At position (5), where the flow was separated, all the models under-predicted the velocity. However, the new model with the fine grids and the DES Realizable k-ε model did better than the other models. The v2f-Dav model failed primarily because the Reynolds averaging may not be appropriate for a separated flow. The LES-DSL model failed to predict good results since it requires a finer grids than DES. This also reflects the advantage of the DES models. At position (3), all the models predicted similar results, though small discrepancies could be found for all the models.

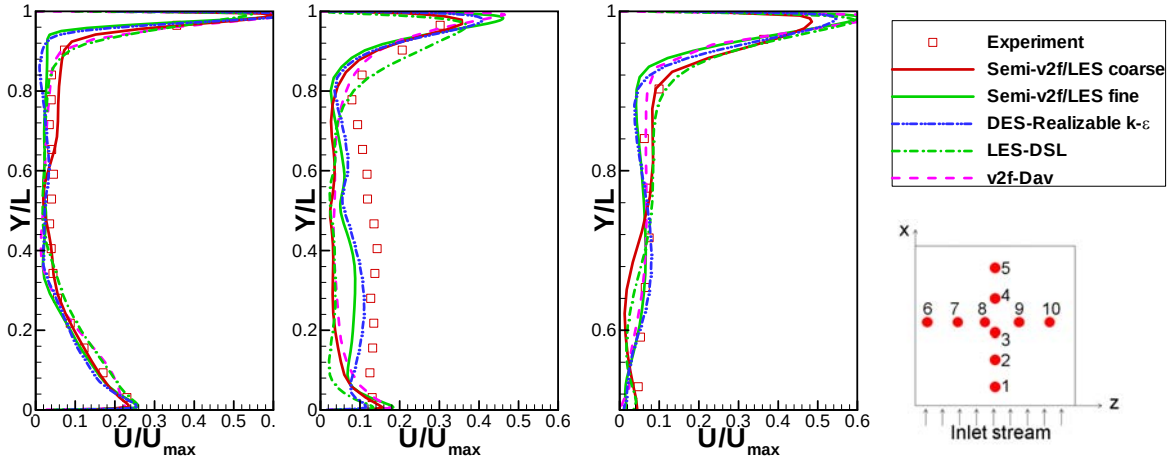

Best Position (6) Worst Position (5) Average Position (3)

Figure 3 Air velocity profiles predicted by the Semi-v2f/LES model for the mixed convection flow (a) best position, (b) worst position, and (c) average position. (Square symbols: experiment; red solid lines: Semi-v2f/LES with the coarse grids; green solid lines: Semi-v2f/LES with the fine grids; dash dot-dot lines: DES realizable k-ε; dash dot lines: LES-DSL; dash lines: v2f-Dav.)

Figure 4 shows the temperature prediction by the models. At position (8), the new model with the coarse grids surprisingly predicted better results, compared with the other models. The new model with the fine grids also predicted slightly better results than the Realizable k-ε model and the v2f-Dav model. The results of the LES-DSL model were comparable with those of the new model with the fine grids. At position (4), the results by the new model with the two grid distributions were better than those by the other models. At position (5), the new model with the fine grids predicted one of the best profiles. The new model with the coarse grids predicted an incorrect peak at Y/L=0.6. The grid distribution of 44x44x44 was not fine enough for the new model to capture the separated flow.

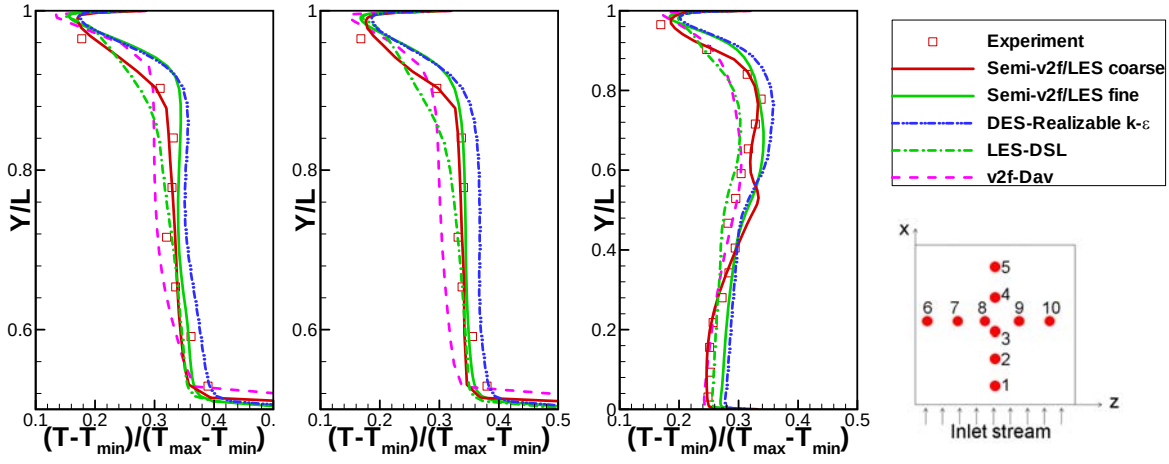

Best Position (8) Worst Position (4) Average Position (5)

Figure 4 Air temperature profiles predicted by the Semi-v2f/LES model for the mixed convection flow (a) best position, (b) worst position, and (c) average position. (Square symbols: experiment; red solid lines: Semi-v2f/LES with the coarse grids; green solid lines: Semi-v2f/LES with the fine grids; dash dot-dot lines: DES realizable k-ε; dash dot lines: LES-DSL; dash lines: v2f-Dav.)

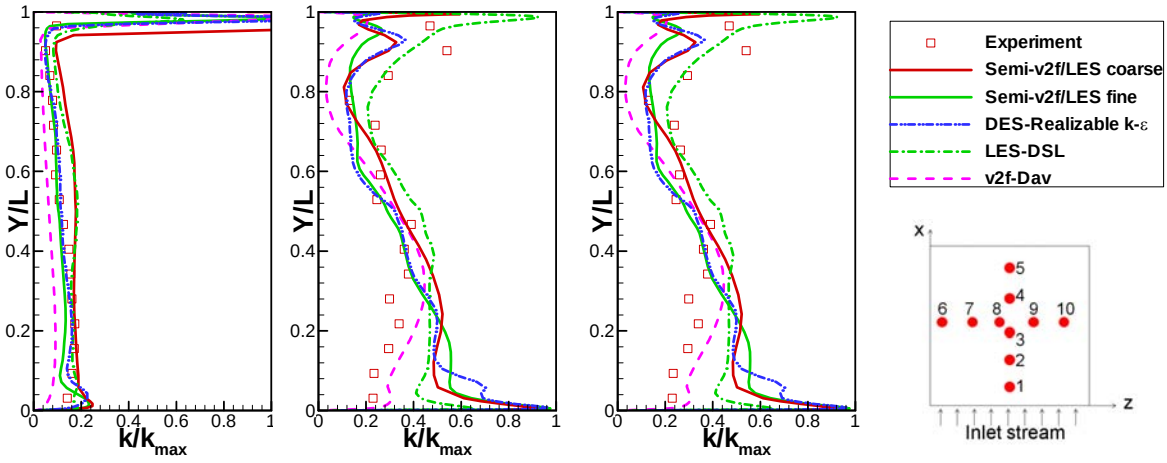

Best Position (1) Worst Position (5) Average Position (10)

Figure 5 Turbulence kinetic energy profiles predicted by the Semi-v2f/LES model for the mixed convection flow (a) best position, (b) worst position, and (c) average position. (Square symbols: experiment; red solid lines: Semi-v2f/LES with the coarse grids; green solid lines: Semi-v2f/LES with the fine grids; dash dot-dot lines: DES realizable k-ε; dash dot lines: LES-DSL; dash lines: v2f-Dav.)

Figure 5 shows the turbulence kinetic energy profiles predicted by the four models. The new model with the fine grids predicted the best result at position (1). The DES Realizable k-ε model performed similarly. The LES-DSL model significantly over-predicted the turbulence level, while the v2f-Dav model under-predicted it. At position (5), none of the four models predicted well the turbulence kinetic energy. It is indeed difficult to capture the fluctuating flow where the flow was highly separated. At position (10), where most models showed average performance, the LES-DSL model was slightly better.

3.2 Strong Buoyancy-Driven Flow

The second case tested was a strong buoyancy-driven flow in a fire room. This case was chosen for studying the robustness of the new model. The case was designed by Murakami et al. (1995), who measured detailed fluctuating velocity using two-component laser doppler velocimetry (LDV), and the temperature using thermal couples. The test room was 5.9 ft (1.8 m) long, 3.9 ft (1.2 m) wide, and 3.9 ft (1.2 m) high as shown in Figure

6. A total of 9.1 kW of heat source was placed at the corner of the room. The surface temperature at the heat source reached more than 932ºF (500ºC). An opening of size 1.3 x 3.0 ft (0.4 x 0.9 m) connected the air between the test room and the outside chamber. The fluctuating velocity and temperature were measured at 12 lines at two sections.

The numerical simulations calculated the air inside the test room as well as the outer enclosure that is a very large laboratory. This helped to avoid instability in using a pressure boundary condition for the opening. The measured surface temperature was used as boundary conditions for the simulations. Due to the high temperature difference between the heat source surface and ambient air, the Boussinesq approximation is no longer valid. Instead, the ideal gas law was used for determining the air density:

$$\rho = \frac{P_{op}}{RT} \tag{3.1}$$

where, P_{op} is the pressure at the opening, R is the gas constant, and T is the air temperature.

The use of variable density would change the form of equations presented in section 2. Since typical indoor airflow is with small temperature difference, it is much better to use the equations given in section 2. This case is an exceptional case so this paper omitted the differences on the governing equations.

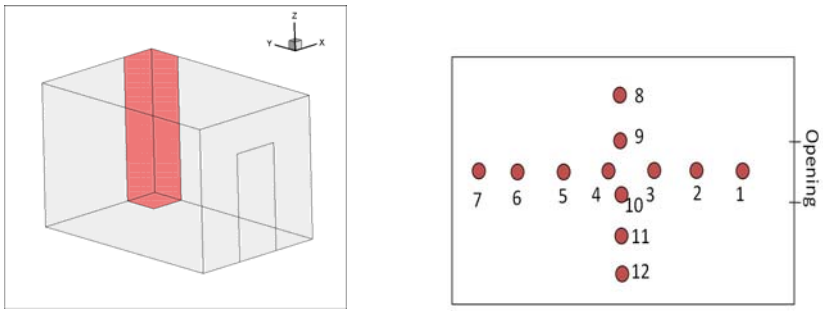

Figure 6 Schematic of the case with strong buoyancy-driven flow (Murakami et al., 1995)

Although this case was primarily used to test the robustness of the new model, the results from the DES Spalart-Allmaras (DES-SA) model and the LES-DSL model are included for comparison. The test was based on the comparison of the air velocity, air temperature, and the root-mean-square (RMS) velocity predicted. The RMS reflects the turbulence predicted by the models. The results at all 12 measurement lines were compared, but only those at lines 2, 4, and 6 are shown here due to limited space.

Figure 7 depicts the calculated and measured velocity profiles in x-direction. All the models were stable in this extreme case. The Semi-v2f/LES model predicted comparable results as the other models.

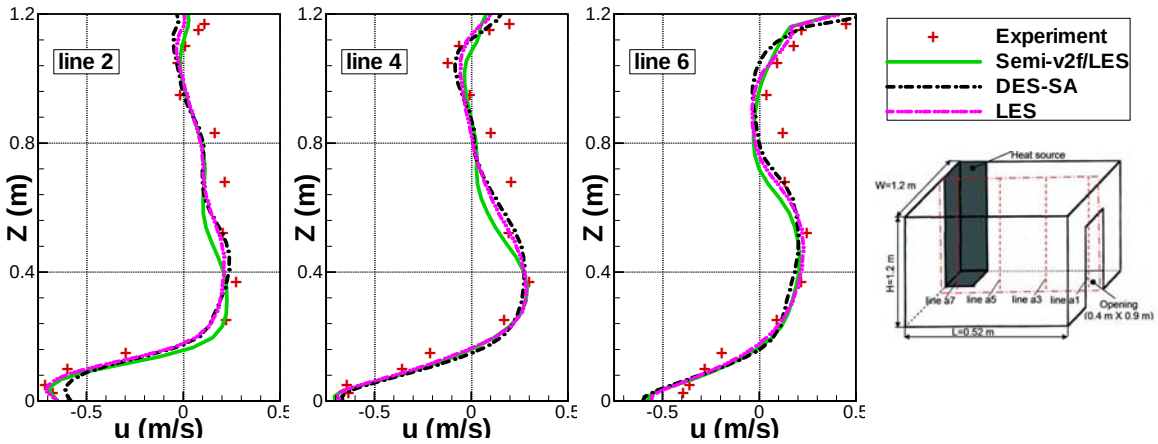

Figure 7 Comparison of the predicted and measured air velocity profiles at x-direction (Plus symbols: experiment; solid lines: Semi-v2f/LES; dash dot lines: DES-SA; dash dot-dot lines: LES-DSL)

Figure 8 compares the predicted and measured air temperature profiles. It is not surprising that all the models predicted reasonable results due to their correct velocity predictions. However, all the models under-predicted the temperature near the ceiling. The Semi-v2f/LES model performed relatively better than the other models due to its better turbulence viscosity formulation in the near wall region.

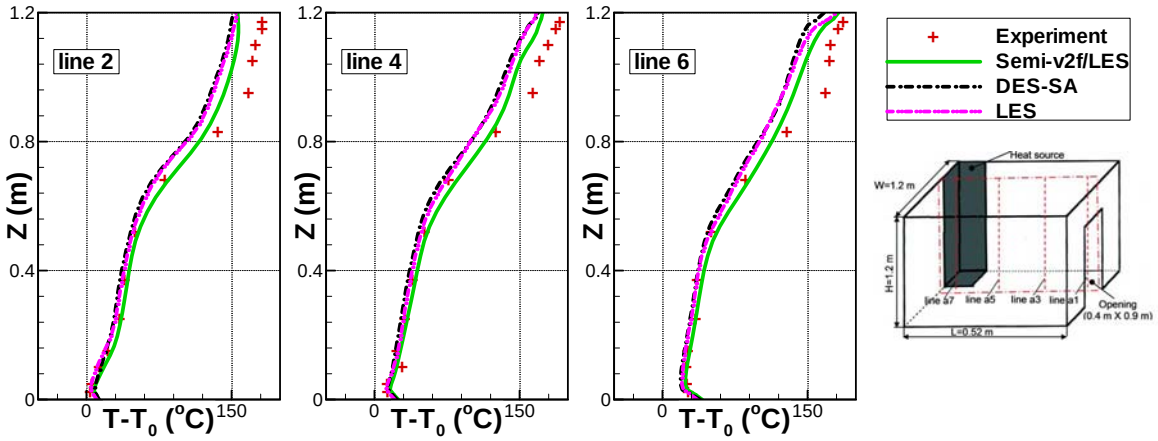

Figure 8 Comparison of the predicted and measured air temperature profiles (Plus symbols: experiment; solid lines: Semi-v2f/LES; dash dot lines: DES-SA; dash dot-dot lines: LES-DSL)

Figure 9 shows the root-mean-square velocity profiles at x-direction. This flow quantity was obtained statistically using the solution at each time step. Although, it is more

difficult to get good agreement for the second-order momentum than the first-order one, the three models used were able to predict the correct trend of the profile. The DES-SA model predicted poorer results than the other two models because the model solved only one turbulence transport quantity, the modified turbulence viscosity, could not calculate the turbulence length scale related to the local shear layer thickness. Therefore, the model may not be accurate for a complicated shear flow. The new Semi-v2f/LES model and LES-DSL model had comparable performances.

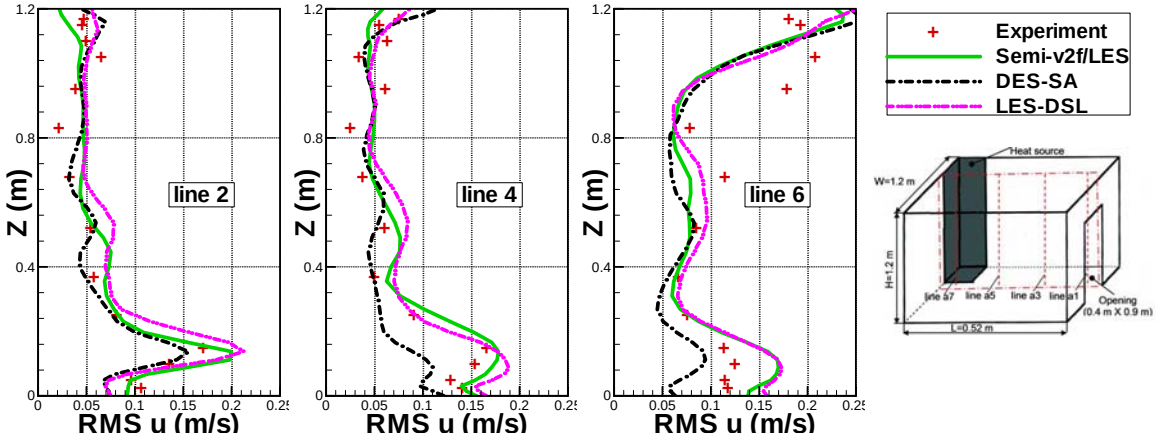

Figure 9 Comparison of the predicted and measured RMS velocity profiles at x-direction (Plus symbols: experiment; solid lines: Semi-v2f/LES; dash dot lines: DES-SA; dash dot-dot lines: LES)

The computational cost of the new model was very similar to the DES Realizable model, since they both solved two additional equations for turbulence. The DES-SA model cost slightly less computational time, since it only solved one additional equation for turbulence. The LES-DSL model had simpler formulation than the new model, but required much finer grid near the wall for full LES simulation. Thus, it could cost much higher computational time.

4 EQUATION SECTION (NEXT)CONCLUSIONS

This investigation developed a new RANS/LES hybrid model, the Semi-v2f/LES model, for indoor airflow simulations. The development simplified the v2f model by replacing the partial differential equation for $\overline{v'^2}$ and f with an algebraic equation for $\overline{v'^2}$.

The study tested the performance of the Semi-v2f/LES model by applying it to predict mean and turbulence quantities in two indoor airflows. The first case was a mixed

convection flow in a model room with typical indoor airflow features. The new model predicted the best turbulence kinetic energy results and comparable velocity and temperature results among several models tested. The second case was a strong buoyancy-driven flow in a room. The new model performed well in this case. It gave the best temperature prediction and was one of the best models for turbulence predictions.

REFERENCES:

Akselvoll, K. and Moin, P. 1992. Large eddy simulation of a backward facing step flow. *Engineering Turbulence Modeling and Experiments 2*, (Rodi, W. and Martelli, F. eds.), Elsevier, 303-313.

Costa, J.J., Oliveira, L.A. and Blay, D. 1999. Test of several versions for the k-ε type turbulence modelling of internal mixed convection flows. *International Journal of Heat and Mass Transfer*, 42(23):4391–409.

Davidson, L., Nielsen, P.V. and Sveningsson, A. 2003. Modification of the v2f model for computing the flow in a 3D wall jet. *Turbulence, Heat and Mass Transfer* 4:577-84.

Davidson, L., Peng, S.H. 2003. Hybrid LES-RANS modelling: a one-equation SGS model combined with a k–x model for predicting recirculating flows. *Int. J. Numer. Methods Fluids* 43, 1003–1018.

Durbin, P.A. 1991. Near-wall turbulence closure modeling without 'damping functions'. *Theoretical and Computational Fluid Dynamics*, Vol. 3(1), 1 - 13.

FLUENT 6.2 (2003) User's Guide, FLUENT Inc.

Forsythe, J. R.. Squires K. D., Wurtzler K. E. and Spalart P. R. 2004. Detached-eddy simulation of the F-15E at high alpha. *Journal of aircraft* vol. 41, no2, 193-200

Gadgil, A.J., C. Lobscheid, M.O. Abadie, and E.U. Finlayson. 2003. Indoor pollutant mixing time in an isothermal closed room: An investigation using CFD. *Atmospheric Environment* 37(39–40):5577–586.

Georgiadis, N.J., Alexander, J.I.D., and Reshotko, E. 2003. Hybrid Reynolds-averaged Navier–Stokes/large-eddy simulations of supersonic turbulent mixing. *AIAA Journal.* 41, 218–229.

Hamba, F. 2001. An attempt to combine large eddy simulation with the k–ε model in a channel-flow calculation. *Theoret. Comput. Fluid Dyn.* 14, 323–336.

Hamba, F. 2003. A hybrid RANS/LES simulation of turbulent channel flow. *Theoret. Comput. Fluid Dyn.* 16, 387–403.

Holmes, S.A., A. Jouvray, and P.G. Tucker. 2000. An assessment of a range of turbulence models when predicting room ventilation. *Proceedings of Healthy Buildings* 2000 2:401–06.

Hsieh, K.J., and F.S. Lien. 2004. Numerical modeling of buoyancy-driven turbulent flows in enclosures. *International Journal of Heat and Fluid Flow* 25:659–70.

Kawai, S., Fujii, K. 2005. Computational study of a supersonic base flow using hybrid turbulence methodology. *AIAA Journal.* 43, 1265–1275.

Le, H., Moin, P., Kim, J. 1997. Direct numerical simulation of turbulent flow over a backward-facing step. *J. Fluid Mech*. 330, 349–374.

Menter, F. R., Kuntz, M., and Langtry, R. 2003. Ten Years of Experience with the SST Turbulence Model. In K. Hanjalic, Y. Nagano, and M. Tummers, editors, *Turbulence, Heat and Mass Transfer* 4:625-632. Begell House Inc.

Murakami, S., Kato, S., and Yoshie, R. 1995, Measurement of turbulence statistics in a mode fire room by LDV. *ASHRAE Transactions*, Vol. 101, 287 - 301.

Smagorinsky, J. 1963. General Circulation Experiments with the Primitive Equations. I. The Basic Experiment. *Month. Wea. Rev.*, 91:99-164.

Spalart, P.R., W.H. Jou, M. Stretlets, and S.R. Allmaras. 1997. Comments on the feasibility of LES for wings and on the hybrid RANS/LES approach. *Proceedings of the First AFOSR International Conference on DNS/LES*, Ruston, LA.

Strelets, M. 2001. Detached Eddy Simulation of Massively Separated Flows. *AIAA, Aerospace Sciences Meeting and Exhibit*, 39 th. Reno, NV.

Tucker, P., Davidson, L. 2004. Zonal k-l based large eddy simulations. *Computers and Fluids 33*, 267–287.

Wang, M., and Chen, Q. 2009. Assessment of Various Turbulence Models for Flows in Enclosed Environment (RP-1271). *HVAC&R Research*, 15(6), 1099-1119.

Wilcox, D. C. 2006. Turbulence Modeling for CFD. DCW Industries, Inc, La Canada, CA

Yuan, X., Chen, Q., Glicksman, L.R., Hu, Y., and X. Yang. 1999. Measurements and computations of room airflow with displacement ventilation. *ASHRAE Transactions*, 105(1), 340-352.

Zhai, Z.Q., Zhang, W., Zhang, Z., and Chen, Q. 2007. Evaluation of various turbulence models in predicting airflow and turbulence in enclosed environments by CFD: part 1 - Summary of prevalent turbulence models. *HVAC&R RESEARCH* 13 (6):853-870.

Zhang, Z., Zhai, Z.Q., Zhang, W., and Chen, Q. 2007 Evaluation of various turbulence models in predicting airflow and turbulence in enclosed environments by CFD: Part 2-comparison with experimental data from literature. *HVAC&R RESEARCH* 13(6): 871-886.

APPENDIX

This appendix provides all the equations for the Semi-v2f/LES model. The transport equation for k is:

$$\frac{\partial}{\partial t}(\rho k)+\frac{\partial}{\partial x_j}(\rho k u_j)=\frac{\partial}{\partial x_j}\left[\left(\mu+\frac{\mu_t}{\sigma_k}\right)\frac{\partial k}{\partial x_j}\right]+G_k+G_b-\rho\varepsilon-Y_M+S_k$$

The transport equation for ε is:

$$\frac{\partial}{\partial t}(\rho\varepsilon)+\frac{\partial}{\partial x_j}(\rho\varepsilon u_j)=\frac{\partial}{\partial x_j}\left[\left(\mu+\frac{\mu_t}{\sigma_\varepsilon}\right)\frac{\partial\varepsilon}{\partial x_j}\right]+\rho C_1 S_\varepsilon-\rho C_2\frac{\varepsilon^2}{k+\sqrt{\nu\varepsilon}}+C_{1\varepsilon}\frac{\varepsilon}{k}C_{3\varepsilon}G_b+S_\varepsilon$$

The algebraic equation for $\overline{v'^2}$ is:

$$\overline{v'^2}=0.308\left[1-\exp\left(-\frac{y^*}{50.836}\right)\right]k$$

The turbulence viscosity is determined by:

$$\nu_t=\min\left\{0.07\frac{k^2}{\varepsilon},0.22\overline{v'^2}T\right\}=\nu_t=0.07\min\left\{\frac{k^2}{\varepsilon},\left[1-\exp\left(-\frac{y^*}{50.836}\right)\right]\cdot T\right\}$$

where:

$$T=\min\left\{2.0\frac{L}{\sqrt{k}},\max\left[\frac{k}{\varepsilon},6\left(\frac{\overline{v'^2}}{\varepsilon}\right)^{1/2}\right]\right\}$$

and:

$$L=C_L\min\left\{\frac{k^{3/2}}{\varepsilon},V_{CELL}^{1/3}\right\}$$

The terms in k and ε equations:

$$G_k=\mu_t S^2$$

where

$$S=\sqrt{2S_{ij}S_{ij}}$$

$$G_b=-g_i\frac{\mu_t}{\rho\,\mathrm{Pr}_t}\frac{\partial\rho}{\partial x_i}$$

$$Y_k=\frac{\rho k^{3/2}}{l_{DES}}$$

where

$$l_{DES} = \min(l_{rke}, l_{LES})$$

$$l_{rke} = \frac{k^{3/2}}{\varepsilon}$$

$$l_{LES} = C_{DES}\Delta$$

$$C_1 = \max\left[0.43, \frac{\eta}{\eta+5}\right],\ \eta = \mathrm{S}\frac{\mathrm{k}}{\varepsilon},$$

Model constant is:

$C_{1\varepsilon} = 1.44$, $C_2 = 1.9$, $\sigma_k = 1.0$, $\sigma_\varepsilon = 1.2$, $C_{DES} = 0.61$.